THE ASTROPHYSICAL JOURNAL LETTERS, 749:L34 (6pp), 2012 April 20 doi:10.1088/2041-8205/749/2/L34

A WARM MODE OF GAS ACCRETION ON FORMING GALAXIES

GIUSEPPE MURANTE[1,2], MATTEO CALABRESE[3], GABRIELLA DE LUCIA[4], PIERLUIGI MONACO[2,4], STEFANO BORGANI[2,5,6], AND KLAUS DOLAG[7]

[1] Osservatorio di Torino, Strada Osservatorio 20, I-10025, Pino Torinese (TO), Italy; murante@oato.inaf.it
[2] Dipartimento di Fisica - Sezione di Astronomia, Università di Trieste, via Tiepolo 11, I-34131 Trieste, Italy; monaco@oats.inaf.it, borgani@oats.inaf.it
[3] Dipartimento di Fisica Generale "Amedeo Avogadro," Università degli Studi di Torino, Via P. Giuria 1, I-10125, Torino, Italy; calabrese@oato.inaf.it
[4] I.N.A.F, Osservatorio di Trieste, Via Tiepolo 11, I- 34131, Trieste, Italy; delucia@oats.inaf.it
[5] I.N.A.F, Osservatorio Astronomico di Trieste, Via Tiepolo 11, I- 34131, Trieste, Italy
[6] I.N.F.N, Sezione di Trieste, Trieste, Italy
[7] University Observatory München, Scheinerstr. 1, 81679, München, Germany; kdolag@mpa-garching.mpg.de
Received 2011 October 26; accepted 2012 February 17; published 2012 April 2

ABSTRACT

We present results from high-resolution cosmological hydrodynamical simulations of a Milky-Way-sized halo, aimed at studying the effect of feedback on the nature of gas accretion. Simulations include a model of interstellar medium and star formation, in which supernova (SN) explosions provide effective thermal feedback. We distinguish between gas accretion onto the halo, which occurs when gas particles cross the halo virial radius, and gas accretion onto the central galaxy, which takes place when gas particles cross the inner one-tenth of the virial radius. Gas particles can be accreted through three different channels, depending on the maximum temperature value, $T_{\rm max}$, reached during the particles' past evolution: a cold channel for $T_{\rm max} < 2.5 \times 10^5$ K, a hot one for $T > 10^6$ K, and a warm one for intermediate values of $T_{\rm max}$. We find that the warm channel is at least as important as the cold one for gas accretion onto the central galaxy. This result is at variance with previous findings that the cold mode dominates gas accretion at high redshift. We ascribe this difference to the different SN feedback scheme implemented in our simulations. While results presented so far in the literature are based on uneffective SN thermal feedback schemes and/or the presence of a kinetic feedback, our simulations include only effective thermal feedback. We argue that observational detections of a warm accretion mode in the high-redshift circumgalactic medium would provide useful constraints on the nature of the feedback that regulates star formation in galaxies.

Key words: galaxies: evolution – galaxies: formation – methods: numerical

Online-only material: color figures

1. INTRODUCTION

In the current standard picture for structure formation, galaxies are believed to form from condensation of gas within the potential wells of dark matter (DM) halos (White & Rees 1978). Therefore, understanding how gas is accreted onto DM halos and galaxies is crucial to understand the process of galaxy formation.

Substantial numerical work recently focused on the "cold accretion" mode (Birnboim & Dekel 2003; Keres et al. 2005) as the main driver for gas accretion at high redshift and for halos less massive than a few times 10^{11} $M_\odot$. The distinction between two modes of accretion, cold and hot, was clearly understood when the first hierarchical galaxy formation models were presented (Rees & Ostriker 1977; Binney 1977; see also Benson & Bower 2011). If the halo virial temperature is larger than the temperature of the accreting gas, this will accrete supersonically, which causes the formation of an accretion shock. If the gas cooling time is longer than the dynamical time of the halo, the shock will occur at a radius that is comparable or slightly larger than the virial radius (Bertschinger 1985; Evrard 1990). If the cooling time is much shorter than the halo dynamical time, the shock will occur much closer to the forming galaxy. The gas is still heated to very high temperature, but it cools so rapidly that it cannot maintain the pressure needed to support a quasi-static hot atmosphere.[8]

[8] In recent work, gas in cold flows is also collimated, i.e., it is accreted along cosmic filaments.

This picture has been validated by one-dimensional hydrodynamical simulations (Birnboim & Dekel 2003; see also Forcada-Miro & White 1997), and by recent three-dimensional hydrodynamical simulations (Keres et al. 2005; Ocvirk et al. 2008). These simulations have shown that a static atmosphere of hot, virialized gas develops in halos above 2.3×10^{11} $M_\odot$, and that this "transition mass" is nearly constant as a function of redshift. Simulations have also pointed out that, even when a shock is present, cold gas accretion can occur along filaments that penetrate deep inside the hot halo and might funnel gas to the central galaxy, elevating its star formation rates.

Brooks et al. (2009) investigated gas accretion in a set of high-resolution simulations spanning about two orders of magnitude in halo mass. They find that, for galaxies in the range 0.01 $L_\star$ to $L_\star$, the early growth of the stellar disk is dominated by gas that is not shocked to the virial temperature of the DM halos, and that cold accretion dominates at all times for galaxies less massive than our Milky Way. A high fraction of gas accretion onto halos is found to be smooth, even for the most massive galaxy considered. In a more recent study, van de Voort et al. (2011) used the OverWhelmingly Large Simulations (OWLS; Schaye et al. 2010) to investigate accretion rates onto halos and galaxies, and their dependence on halo mass and redshift. They confirm that hot mode accretion dominates the growth of massive halos, but show that accretion onto galaxies is very sensitive to feedback processes and metal line cooling. In addition, they confirm that gas accretion on the halo is smooth. Finally, Oppenheimer et al. (2010) studied how gas accretion is affected by kinetic feedback. They found that a significant

Table 1
Simulations

Name	$M_{\rm DM}$	$M_{\rm Gas}$	ϵ	$N_{\rm DM}$ & $N_{\rm Gas}$	$M_{\rm vir}$
R1	1.6×10^6	3.0×10^5	0.325	5, 953, 033	2.70×10^{12}
R2	1.7×10^5	3.2×10^4	0.155	55, 564, 205	...

Notes. Column 1: simulation name; Column 2: mass of the dark matter particle, in $h^{-1}\ M_\odot$; Column 3: mass of the gas particle, in $h^{-1}\ M_\odot$; Column 4: Plummer-equivalent softening length at $z = 0$, in h^{-1} kpc. The softening is physical down to redshift $z = 2$, and comoving afterward; Column 5: number of DM and gas particles in the high-resolution region; Column 6: virial mass of the halo, in $h^{-1}\ M_\odot$. Here we define the virial mass as that contained in a radius enclosing a mean overdensity of 200 times the critical density. The simulation R2 was run down to $z = 2.5$ only.

amount of the gas that later form stars has been previously processed through the winds. This *wind channel* is relevant below $z \approx 2$.

In this Letter, we readdress the issue of gas accretion onto the halo and onto the galaxy, taking advantage of high-resolution hydrodynamical simulations of galaxy-size halos. We use our new star formation and feedback algorithm, MUPPI (Murante et al. 2010), which includes an effective thermal feedback but no kinetic feedback. Our aim is to verify whether, in this scheme, gas accretion onto the central part of the halo remains mainly cold and smooth, and whether these results are robust against increasing numerical resolution, well above that adopted in cosmological simulations.

2. NUMERICAL METHODS

2.1. Simulations

We study the accretion of gas onto the *halo* and on its central part, the *galaxy*, using hydrodynamical simulations of galaxy-size halos. Initial conditions were generated by Stoehr et al. (2002) adopting a ΛCDM cosmology, with $\Omega_m = 0.3$, $\Omega_\Lambda = 0.7$, $H_0 = 70$ km s^{-1} Mpc^{-1}, and $\sigma_8 = 0.9$. A "Milky Way" halo was selected from an intermediate-resolution simulation as a relatively isolated halo which suffered its last major merger at $z > 2$, and with approximately the correct peak rotation velocity at $z = 0$. Our simulations include as many gas particles as high-resolution DM particles, and adopt a baryon fraction of $f_b = 0.19$. In Table 1, we list the main numerical parameters of the simulations. The highest resolution simulation (R2) was run down to $z = 2.5$.

Our simulations were carried out using the Tree+SPH code GADGET-3, an improved version of the GADGET-2 code (Springel 2005), by using the star formation and feedback scheme MUPPI (Murante et al. 2010, M10). In this scheme, each star-forming gas particle is described as a multi-phase particle, where cold and hot gas co-exist in pressure equilibrium. Mass and energy fluxes between different phases are described by a system of ordinary differential equations. The molecular fraction of cold gas is estimated using a phenomenological prescription (Blitz & Rosolowsky 2006). Stars explode and inject a fraction $f = 0.3$ of the available supernova (SN) energy as thermal energy in the hot and tenuous gas phase of neighbors. These do not immediately radiate it away because of the hot gas low density. As a result, our scheme provides effective thermal feedback: gas particles inside and near star-forming regions are heated, and escape from their parent structure along the path of minimal resistance (i.e., the direction of lowest density), with velocities up to ≈100 km s^{-1}, giving rise to galactic fountains. We stress that we do not include kinetic feedback. A particle remains in the multi-phase stage for twice the gravitational dynamical time it had when 95% of its cold phase was accumulated. This simulates the formation and disruption of star-forming giant molecular cloud. We refer to M10 for a detailed description of our scheme and for a discussion of the choice of the relevant parameters, which we kept fixed here. Our model has been included in a recent code-comparison project on galaxy formation simulations (Scannapieco et al. 2011).

Our simulations also include a phenomenological description of the UV background (Haardt & Madau 1996), but no chemical evolution of the gas: gas cooling is computed assuming primordial chemical composition.

2.2. Analysis Method

We analyze the thermal history of gas particle accreting *onto the halo*, and *onto the galaxy* by using the following definitions. The *halo* is defined as a sphere centered on the most bound particle, and with virial radius enclosing an overdensity of 200 times the critical density at the redshift of interest. The *galaxy* includes all particles within one tenth of the virial radius. We will see that this distinction is very important, since the gas accreting onto these components can have different properties. To perform our analysis, we used 131 snapshots, roughly equispaced in redshift from $z = 8.3$.

At each snapshot, we selected the most massive progenitor of our $z = 0$ halo, by using a standard friends-of-friends algorithm with linking length $b = 0.16$. We then assumed that a gas particle is accreted onto the halo (galaxy) at a snapshot n if it is part of the halo (galaxy) at the corresponding snapshot but not at the previous one $n - 1$. Each gas particle is then traced back in time, and the highest temperature reached during its past evolution is recorded.

We distinguish gas accreting in three channels: (1) cold gas, made of particles that never reached temperatures larger than $T_{\rm min} = 2.5 \times 10^5$ K; (2) warm gas, composed of particles that were hotter than $T_{\rm min}$ but colder than $T_{\rm max} = 10^6$ K; (3) hot gas, made of particles that reached temperatures larger than $T_{\rm max}$. In previous work, the *warm* channel has been included in the hot one. In this study, we have considered this separate channel to quantify the accretion that occurs at "intermediate" temperatures, that are indicative of feedback from SNe rather than shock heating.

Finally, we identified all self-bound structures at each snapshot using the algorithm SUBFIND (Springel et al. 2001), and built merger trees for all of them using the same procedure described in Springel et al. (2005).

Using these merger trees, we check if gas particles accreted on the halo or on the galaxy belong to a distinct subhalo at the previous time, i.e., for each accretion channel, we determine the fraction of gas accreted in "clumps." Gas particle that were not assigned to a subhalo in the past are considered as "smoothly" accreted.

3. RESULTS

Figure 1 shows the fractional mass accretion rates in the three channels defined above. Right panels are for accretion on the *halo*, while left panels show the corresponding accretion rates on the *galaxy*. We show the accretion rates for the resolution levels R1 and R2, as well as for a R1 run that adopted the Springel & Hernquist (2003) effective model (see below). The figure shows that gas is accreted on the halo mainly via the *cold* channel for

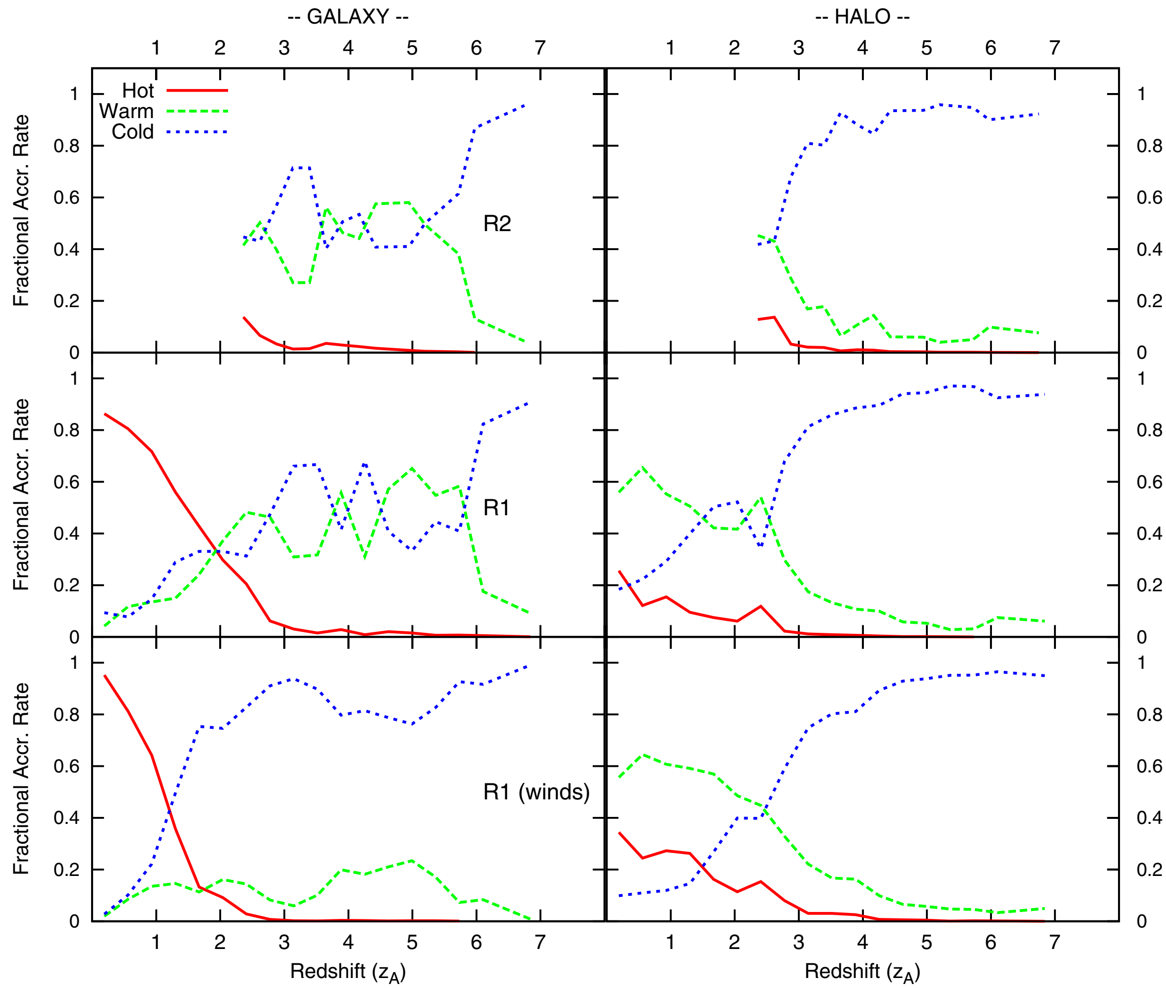

Figure 1. Right panels: gas fractional accretion rates onto the *halo* as a function of the accretion redshift. Left panels: corresponding fractional gas accretion rates onto the *galaxy*. In red we show the hot gas accretion, in green the warm accretion, and in blue the cold accretion. For clarity, we have resampled our redshift outputs in 20 redshift bins.

(A color version of this figure is available in the online journal.)

all runs considered. At low redshift, $z < 2$, the importance of *warm* and *hot* channels increases, in agreement with previous studies (e.g., Keres et al. 2009; Brooks et al. 2009; van de Voort et al. 2011).

Results are quite different for the accretion onto the galaxy. In this case, the *cold* and the *warm* channels equally contribute to gas accretion at high redshift. At later times, the *hot* channel provides the dominant contribution.

Our findings are robust against resolution: our R2 simulation has a mass resolution which is sufficient to resolve halos of $\approx 10^6\ M_\odot$ with $\approx$100 DM particles. Therefore, results from this simulations are reliable also at high redshift and, as shown in Figure 1, they are in excellent agreement with those obtained for the R1 run.

Figure 2 shows density maps of gas which accreted onto the *galaxy* between redshifts $z = 2.5$ and $z = 2.0$. We show the gas at previous redshifts: $z = 3.8$ (left column), $z = 2.9$ (middle column), and $z = 2.5$ (right column), for the R1 simulation. Maps are centered on the most massive progenitor at the corresponding redshift. The upper, middle and lower rows are for the *cold*, *warm*, and *hot* channels, respectively. The figure shows that the cold gas is characterized by a very clumpy distribution, while the hot gas is always diffused around the most massive progenitor. Interestingly, warm gas is more diffuse than cold gas, but it surrounds the cold clumps. This suggests that the infalling cold clumps are strongly star forming, and that they heat and eject part of their gas while infalling toward the central galaxy.

This is confirmed by the analysis of the multi-phase nature of the accreting gas: SN thermal feedback is effective at heating multi-phase particles. So, by computing the fraction of gas particles that were multi-phase when they reached their maximum temperature, one can disentangle the influence of SN heating from gravitational shock heating. For the R1 simulation, averaging over the entire redshift range (from $z = 8.3$ to $z = 0$), we find that when accreting gas reaches its maximum temperature, $\sim$97% of it is multi-phase and star forming in the *cold* channel. The corresponding fractions for the *warm* and *hot* channels are $\sim$66% and $\sim$8%, respectively. This suggests that gas in the *warm* channel is heated by SN feedback, while gas in the *hot* channel is heated by gravitational shocks.

To better illustrate the role of effective thermal feedback we run simulation R1 using the widely used effective model of Springel & Hernquist (2003) for star formation, with kinetic feedback and velocity $v_w = 340$ km s^{-1}.[9] The resulting

[9] We decouple wind particles from ambient gas for 20 kpc or until density drops to one half of SF threshold.

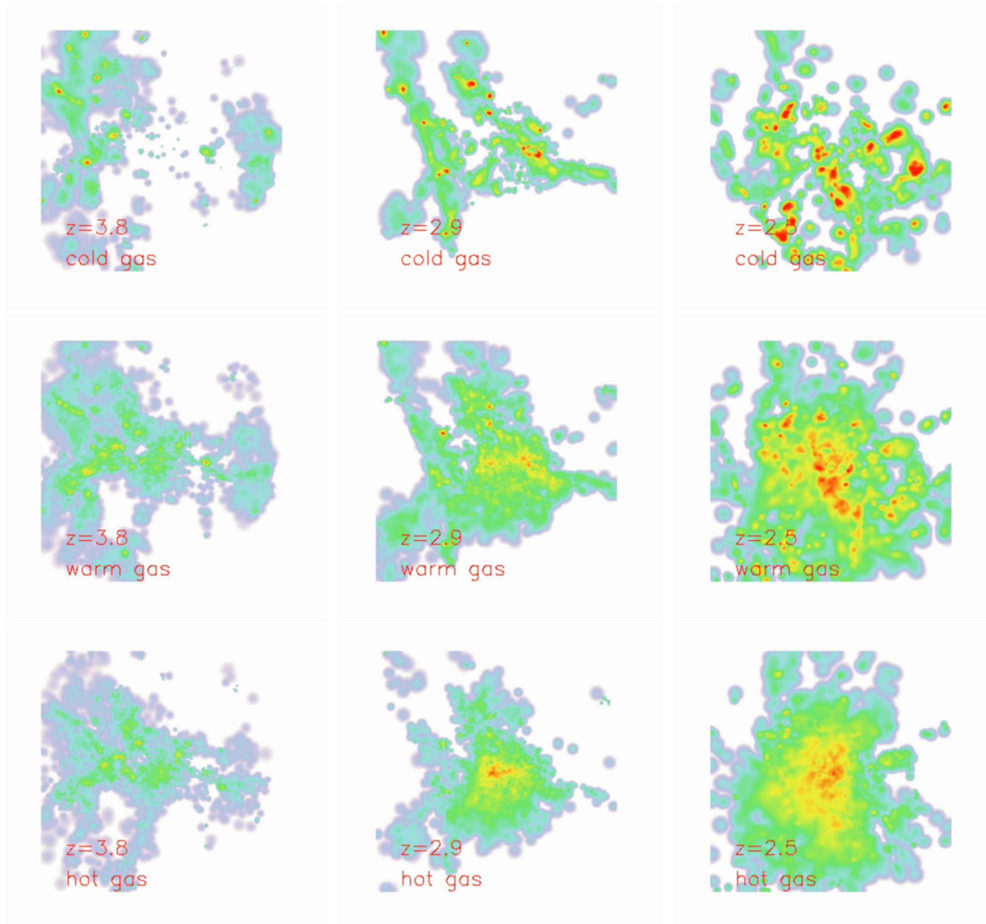

Figure 2. Projected density maps of gas accreting on the *galaxy* between $z = 2.5$ and $z = 2$, for the R1 simulation. Different rows correspond to the three channels considered: cold (upper row), warm (middle row), and hot (lower row). Different columns correspond to different redshifts: $z = 3.8$ (left column), $z = 2.9$ (middle column), and $z = 2.5$ (right column). The scale of the maps are 960, 480, and 240 h^{-1} Mpc comoving for the three columns. The color scale is logarithmic from 1.0 to 10^6 $M_\odot$ h pc^2 comoving (from pale pink to red).

(A color version of this figure is available in the online journal.)

accretion rates are shown in the lower panels of Figure 1: the contribution of the *warm* channel to accretion on the galaxy becomes negligible, while gas accretion in the *cold* channel increases. This confirms that simulations with uneffective thermal feedback are unable to heat cold flows into the warm channel, even when they produce significant outflows.

Finally, for each channel, we analyze the *clumpiness* of gas accretion, both on the *halo* and on the *galaxy* by determining if its particles belonged to an accreting satellite of were accreted smoothly.

Results are shown in Figure 3. For accretion on the halo, we find that *total* gas is mainly smooth (as in, e.g., Brooks et al. 2009, van de Voort et al. 2011). At $z = 0$, 69% of the gas has been accreted smoothly in the R1 simulation. Smooth accretion dominates the *hot* channel, while in the *cold* one, smooth and clumpy accretion contribute equally to the total accretion rate: at $z = 0$ smooth accretion accounts for only 49% of the overall cold accretion.

Also the total accretion rate on the galaxy is mainly smooth, ≈67% for R1, and hot accretion shows the same trend found for the accretion on the halos. We find a significant difference, however, in the *cold* channel. In fact, this channel is dominated by clumpy accretion, with 60% of the gas accreted in this way. The gas accreted through the *warm* channel is also prevalently clumpy.

We stress that the clumps that contribute to the cold and warm channels have a significant (>85%) DM fraction, ruling out possible numerical problems of the SPH technique that can, in certain conditions, produce "cold-gas only" spurious blobs.

4. DISCUSSION AND CONCLUSIONS

We analyzed the gas accretion rate in cosmological numerical simulations of a galaxy-size halo. We take advantage of our new MUPPI star formation and feedback model that provides effective thermal feedback and use different resolution levels to test the robustness of our results.

We distinguished between gas accretion onto the halo (defined as all the matter included in the redshift-dependant virial radius), and accretion onto the central galaxy (defined as all the material included within one tenth of the virial radius). We traced back all gas particles in our simulations, and defined a gas particle to be accreted at redshift z_n if it was not part of the main progenitor (or of its central galaxy) of our $z = 0$ halo at $z_{n-1} > z_n$, but became part of it at z_n. We defined three accretion channels: a cold one, including gas particles whose maximum past temperature was lower than 2.5×10^5 K; a hot channel, which includes gas particles with maximum past temperature larger than 10^6 K; and an intermediate *warm* channel.

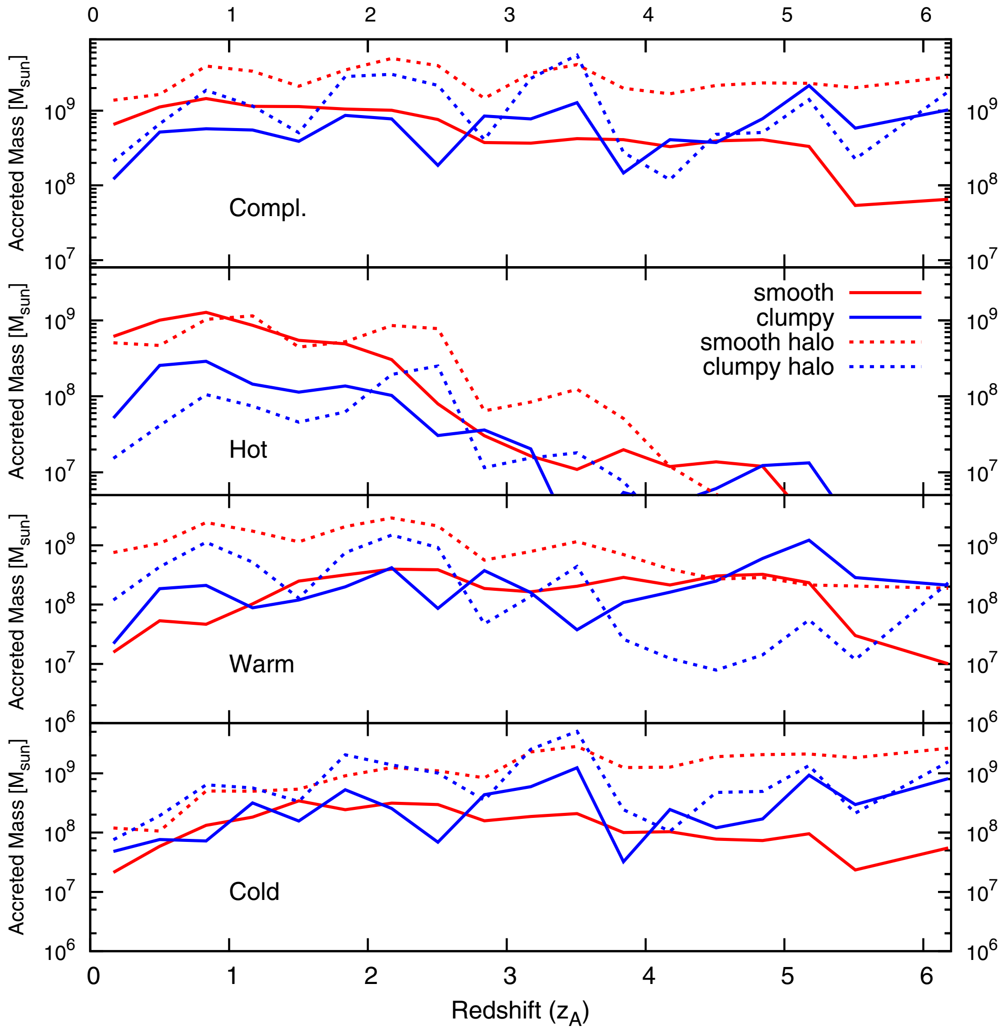

Figure 3. Smooth vs. clumpy accretion for model R1. We show on the *y*-axis the mass accreted between two consecutive redshifts (in $h^{-1}\,M_\odot$) Solid lines refer to accretion on the *galaxy*, while dashed lines are for accretion on the *halo*. Blue and red lines correspond to *clumpy* and *smooth* accretion, respectively. The upper panel shows the total accretion, while the three channels considered are shown in the lower panels: from the second upper to lower panel, accretions for *hot*, *warm*, and *cold* channels.

(A color version of this figure is available in the online journal.)

Our results can be summarized as follows.

1. The *warm* accretion channel becomes as important as the cold one at high redshift, when considering the accretion on the central *galaxy*. This trend is robust against numerical resolution.
2. Gas particles in the *warm* channel are heated by SN feedback. This is confirmed by the analysis of the multiphase nature of the gas, and by the fact that a simulation of the same halo carried out with a model that does not include effective thermal feedback shows negligible accretion rates through this channel.

Regarding the accretion on the halo, our findings confirm previous studies: the "cold" accretion mode on the halo is important at high redshift, while the "hot" accretion mode becomes dominant at lower redshift. However, accretion rates onto the halo are different from accretion rates onto the central galaxy. We find that a significant amount of gas is accreted on the galaxy through a *warm* channel. The gas is in cold clumps when entering the halo, and becomes warm because of the SN feedback originating from star formation within the clumps.

Van de Voort et al. (2011) also analyzed the clumpiness of the accreted gas, but they included all clumps with mass ratio smaller than 1:10 in their smooth component. These clumps are, however, very dense and star-forming, and effectively heat the cold gas to the warm channel.

Oppenheimer et al. (2010) found that a large fraction of low-z star formation experienced a wind phase in the past. However, they studied the effect of *kinetic* feedback, and showed that this channel becomes important below $z = 2$. Their results are thus complementary to those shown in this letter.

The picture emerging from our analysis can be sketched as follow: at high redshift, accreting gas is mainly cold, partly clumpy and partly smooth. Not all of the smooth cold gas reaches the central part of the halos because, behaving as non-collisional material, cold, unshocked gas is not able to loose orbital energy and angular momentum. Thus, only gas streams with very low impact parameters can funnel gas to the central galaxy, contributing to its star formation. Cold clumps suffer dynamical friction and spiral toward the center. Since they are very dense, their star formation rate is high, and part of the gas they contain is heated by SN feedback, and is accreted onto the galaxy as *warm*, slightly less clumpy material. We do not ascribe these findings to specific features of our sub-resolution model, and argue that *any* effective thermal feedback scheme would give similar results. In this picture, the time needed by the cold gas to reach the central galaxy is neither the free fall time nor the cooling time. Smooth cold accreting gas can only reach the galaxy if the impact parameter is small. In contrast, cold clumps are subject to dynamical friction so they can reach the central galaxy even with non negligible impact parameters, over a time-scale that is determined by dynamical friction.

However, the exact quantification of warm flows may well depend on model details. In particular, the entrainment of cold gas into the multi-phase particle may lead to some overestimation of the amount of warm flows. We will address this issue in future work

It is widely accepted that stellar feedback plays an important role in determining the physical properties of galaxies. It remains, however, unclear if the nature of feedback is predominantly kinetic or thermal. Our results demonstrate that stellar feedback strongly affects the thermodynamical state of the gas accreting onto galaxies. In particular, we argue that a mode of feedback that is primarily thermal would produce significant amount of warm gas accreting onto galaxies at high redshift. This has noticeable consequences on the observability of gas flows infalling onto high-redshift galaxies, and may explain, at least in part, why cold flows have been difficult to detect to date.

We acknowledge useful discussions with Matteo Viel. Our simulations were carried out at the "Centro Interuniversitario del Nord-Est per il Calcolo Elettronico" (CINECA, Bologna), with CPU time assigned under two INAF/CINECA grants. The R2 simulation was performed thanks to an INAF-CINECA numerical Key-Project. G.D.L. acknowledges financial support from the European Research Council under the European Community's Seventh Framework Programme (FP7/2007-2013)/ERC grant agreement No. 202781. This work has been partially supported by the European Commission FP7 Marie Curie Initial Training Network CosmoComp (PITN-GA-2009-238356), by PRIN-INAF-2009 grant "Towards an Italian Network for Computational Cosmology," by PRIN-MIUR09 "Tracing the growth of structures in the Universe," and by the INFN PD51 grant.

REFERENCES

Benson, A. J., & Bower, R. 2011, MNRAS, 410, 2653
Bertschinger, E. 1985, ApJS, 58, 39
Binney, J. 1977, ApJ, 215, 483
Birnboim, Y., & Dekel, A. 2003, MNRAS, 345, 349
Blitz, L., & Rosolowsky, E. 2006, ApJ, 650, 933
Brooks, A. M., Governato, F., Quinn, T., Brook, C., & Wadsley, J. 2009, ApJ, 694, 396
Evrard, A. E. 1990, ApJ, 363, 349
Forcada-Miro, M. I., & White, S. D. M. 1997, arXiv:astro-ph/9712204
Haardt, F., & Madau, P. 1996, ApJ, 461, 20
Keres, D., Katz, N., Fardal, M., Davé, R., & Weinberg, D. H. 2009, MNRAS, 395, 160
Keres, D., Katz, N., Weinberg, D. H., & Davé, R. 2005, MNRAS, 363, 2
Murante, G., Monaco, P., Giovalli, M., Borgani, S., & Diaferio, A. 2010, MNRAS, 405, 1491
Ocvirk, P., Pichon, C., & Teyssier, R. 2008, MNRAS, 390, 1326
Oppenheimer, B. D., Davé, R., Keres, D., et al. 2010, MNRAS, 406, 2325
Rees, M. J., & Ostriker, J. P. 1977, MNRAS, 179, 541
Scannapieco, C., et al. 2011, MNRAS, submitted (arXiv:1112.0317)
Schaye, J., Dalla Vecchia, C., Booth, C. M., et al. 2010, MNRAS, 402, 1536
Springel, V. 2005, MNRAS, 364, 1105
Springel, V., & Hernquist, L. 2003, MNRAS, 339, 289
Springel, V., White, S. D. M., Jenkins, A., et al. 2005, Nature, 435, 629
Springel, V., White, S. D. M., Tormen, G., & Kauffmann, G. 2001, MNRAS, 328, 726
Stoehr, F., White, S. D. M., Tormen, G., & Springel, V. 2002, MNRAS, 335, 84
van de Voort, F., Schaye, J., Booth, C. M., et al. 2011, MNRAS, 414, 2458
White, S. D. M., & Rees, M. J. 1978, MNRAS, 183, 341